GEOCHEMICAL CONSTRAINTS ON POTENTIAL UOC CHONDRULE GENESIS BY HYPERVELOCITY IMPACT VAPOR PLUMES AND LIKELY PRECURSOR SOURCES. D. Sheikh[1], M. Humayun[1], [1]National High Magnetic Field Laboratory and Department of Earth, Ocean & Atmospheric Science, Florida State University, Tallahassee, FL 32310, USA (ds18g@my.fsu.edu).

Introduction: Recent work on hypervelocity impacts between solid planetesimals driven by excitation from the inward migration of Jupiter [1, 2] has shown that the resulting impact plumes are dominated by silica-rich vapor. These impact vapor plumes created by collisions between solid planetesimals while in the presence of nebular gas create micro-environments with rapidly changing fO_2, and have been suggested to be feasible environments for chondrule formation before the dissipation of nebular gas from the disk [3, 4]. Chondrules from CB chondrites have distinctive refractory element fractionations (Th/Sc) and volatility-driven Ce and U anomalies that indicate formation from differentiated precursors in an impact vapor plume [5]. The relatively young ages of CB chondrites imply formation after nebular gas had already dissipated [6]. For G chondrites, the presence of volatility-driven Ce and Eu anomalies in Sierra Gorda 009 [7] and Hf-W ages from NWA 5492 [8] suggests that G chondrite chondrules formed from an impact vapor plume under variable fO_2, while nebular gas was still present. The similar ages of unequilibrated ordinary chondrite (UOC) [9] chondrules may suggest that they could have formed by a similar process, so obtaining trace element abundances of UOC chondrules would be useful to test this chondrule forming model.

Evidence for internal fractionation of trace elements driven by mesostasis and/or low-Ca pyroxene remelting and primary feldspar crystallization in UOC chondrules has highlighted the importance of obtaining bulk compositions of UOC chondrules to avoid misinterpretation [10]. However, obtaining a representative bulk chondrule composition is extremely challenging particularly in UOCs. Many elements are incompatible in olivine, and somewhat incompatible in pyroxenes, so incompatible element analysis in large spots would be dominated by mesostasis, which should provide an effective proxy for measuring bulk chondrule ratios of incompatible elements. To better understand the formation of UOC chondrules, we analyzed individual chondrules from NWA 7731 (L3.00), NWA 10061 (LL3.00), NWA 12213 (LL/L3.2), and NWA 3358 (H3.10), with the goal of determining potential chondrule precursor sources and chondrule forming processes [11]. Here, we apply the results to new models.

Analytical Methods: Back-scattered electron images of 153 chondrules from four UOC sections were obtained under high vacuum setting with an accelerating voltage of 15 kV and a working distance of 6.0 mm with a 2010 FEI Nova 400 NanoSEM scanning electron microscope (SEM) at Florida State University to identify the textures and the silicate phases present within each chondrule. Chondrules were subsequently analyzed for 53 elements utilizing a New Wave™ UP193FX laser ablation ICP-MS at FSU [5, 12]. Measurements were conducted using 100 µm spot sizes, 10 second dwell time, and a 50 Hz repetition rate. Multiple spots were taken within each chondrule and averaged.

Results: Ce, Eu and Yb anomalies are plotted for each of the 153 chondrules analyzed (Fig. 1A-B). Most chondrules plotted display prominent Ce and Eu anomalies. Some chondrules show resolvable, but small (±15%), Yb anomalies.

Fig. 2 displays Zr/Hf and Nb/Ta ratios for UOC and Gujba chondrules [5, 11], and for eucrites [15]. Most chondrules scatter around chondritic ratios for Zr/Hf and Nb/Ta. Six of the 7 measured Al-rich chondrules plot on a trend extending from Nb/Ta ratios of 3 to 22 at a relatively constant Zr/Hf ratio.

Abundances of Zr and Th are plotted for UOC and Gujba chondrules [5, 11], and for eucrites [15] (Fig. 3). Most chondrules from this study exhibit chondritic Zr/Th ratios.

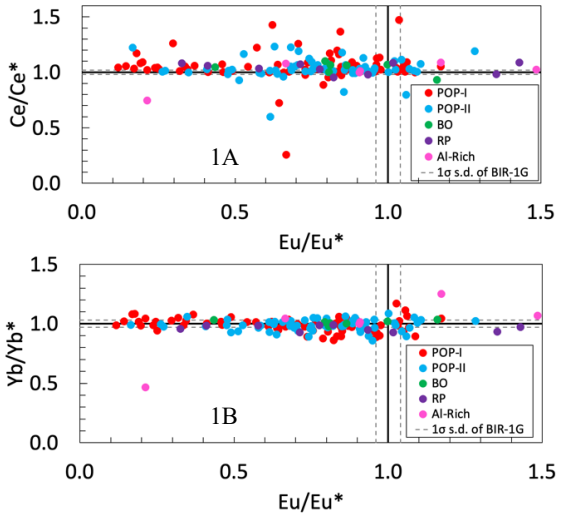

Fig. 1: *Cerium anomaly (Ce/Ce*) and Yb anomaly (Yb/Yb*) plotted vs. Eu anomaly (Eu/Eu*) (1A-B). Error bands (1σ) plotted as dashed lines show the reproducibility of BIR-1G. CI normalization from [13].*

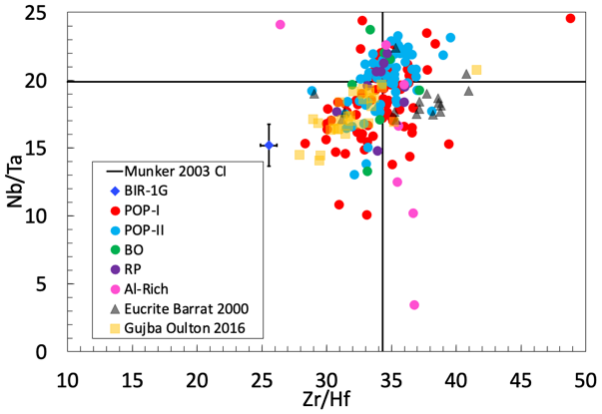

Fig. 2: *Zr/Hf and Nb/Ta ratios for UOC and Gujba chondrules [5, 11], and eucrites [15]. Lines show CI values [14]. Error bars on BIR-1G are representative for all UOC chondrules analyzed in this study.*

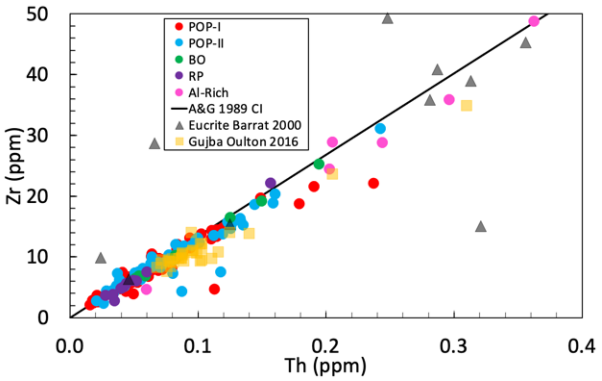

Fig. 3: *Th and Zr abundances for UOC and Gujba chondrules [5, 11], and eucrites [18]. Line: CI [13].*

Discussion: The initial vapor plume of a planetesimal impact is expected to be highly oxidizing due to silicate vaporization [2]. At a later stage, after expansion into nebular gas, hydrogen mixes into the plume creating reducing conditions for the still hot recondensing droplets [3, 4]. Anomalies of Ce, Eu, and Yb are volatility driven as Ce anomalies form under oxidizing conditions due to the volatility of Ce^{+4} [16], while Eu and Yb anomalies form under reducing conditions due to the volatilities of Eu^{+2} and Yb^{+2} [17]. The presence of Ce anomalies in most chondrules suggests that fO_2 conditions were oxidizing for at least some duration during their formation. Vaporized Ce^{+4} encountering H_2 would be reduced to refractory Ce^{+3}, again. Negative Ce anomalies represent residual melt droplets, while positive Ce anomalies represent small droplets that recondensed Ce from the vapor phase. The large range of Eu anomalies present in most chondrules, compared to the relatively small deviations in Yb anomalies implies that fO_2 conditions during the chondrule forming event were not as reducing as canonical solar nebula values [18]. Therefore, UOC chondrules must have formed under conditions where fO_2 conditions varied from oxidized to reduced, compatible with formation inside of impact vapor plumes that mix with nebular H_2 gas [3, 4].

Highly refractory elements Zr, Hf, Nb, and Ta are unlikely to fractionate during evaporation or condensation processes. Geochemical twins Zr/Hf and Nb/Ta differ slightly in their compatibility with Zr and Nb being more incompatible. Therefore, correlations between Zr/Hf and Nb/Ta are suggestive of inheritance from a differentiated precursor. In Fig. 2, Type-II UOC chondrules are indistinguishable from CI ratios, but Type-I chondrules plot below the CI ratios along the Gujba trend [5]. Most Al-rich chondrules are distinct, exhibiting Nb/Ta ratios at a relatively constant Zr/Hf ratio (Fig. 2). Under reducing conditions, Nb has been observed to partition into sulfide phases [19], but such conditions are unlikely to have occurred during the chondrule forming event since fO_2 was not low enough to create substantial Yb anomalies. Rather, Al-rich chondrules must have inherited the Nb depletion from their precursors, possibly from refractory inclusions [20, 21].

A few UOC chondrules display fractionated Zr/Th, suggesting differentiated precursors, but most UOC chondrules display chondritic Zr/Th, implying that most UOC chondrules formed from undifferentiated precursors (Fig. 3).

References. [1] Carter P. J., and Stewart S. T. (2020) *PSJ, 1:45*, 1-23. [2] Davies E. J. et al. (2020) *JGR, 125*, 1-17. [3] Stewart S. T., et al. (2019) *LPSC 50,* abstract #1251. [4] Choksi N. et al. (2020) *MNRAS, 000*, 1-16. [5] Oulton J. et al. (2016) *GCA, 177,* 254-274. [6] Krot A. N. et al. (2005) *Nature, 436*, 989-992. [7] Ivanova M. A. et al. (2020) *MaPS, 55*, 1764-1792. [8] Friend P. et al. (2011) *LPSC 42*, abstract #1095. [9] Connelly J. N. et al. (2012) *Science, 338*, 651-655. [10] Pape J. et al. (2021) *GCA, 292*, 499-517. [11] Sheikh D., and Humayun M. (2020) *LPSC 51,* abstract #1345. [12] Yang S. et al. (2018) *G³ 19,* 4236-4259. [13] Anders E., and Grevesse N. (1989) *GCA, 53,* 197-214. [14] Munker C. et al. (2003) *Science, 301,* 84-87. [15] Barrat J. et al. (2000) *MaPS, 35,* 1087-1100. [16] Wang J. et al. (2001) *GCA, 65,* 479-494. [17] Davis A. M., and Grossman L. (1979*) GCA,* 43, 1611-1632. [18] Grossman L. et al. (2008) In (Macpherson G. J. et al. eds.) Oxygen in the Solar System, *Rev. Min Geochem. 68*, 93-140. [19] Humayun M., and Campbell A. J. (2003) *LPSC 34,* abstract #1480. [20] Grossman J. N., and Wasson J. T. (1983) *GCA, 47,* 759-771. [21] Bischoff A., and Keil K. (1984) *GCA, 48,* 693-709.